A connection between the Camassa-Holm equations and turbulent flows in channels and pipes

S. Chen[1], C. Foias[1,2], D.D. Holm[1], E. Olson[1,2], E.S. Titi[3,4], S. Wynne[3,4]

Abstract. In this paper we discuss recent progress in using the Camassa-Holm equations to model turbulent flows. The Camassa-Holm equations, given their special geometric and physical properties, appear particularly well suited for studying turbulent flows. We identify the steady solution of the Camassa-Holm equation with the mean flow of the Reynolds equation and compare the results with empirical data for turbulent flows in channels and pipes. The data suggests that the constant α version of the Camassa-Holm equations, derived under the assumptions of isotropy and homogeneity, holds to order α distance from the boundaries. Near a boundary, these assumptions are no longer valid and the length scale α is seen to depend on the distance to the nearest wall. Thus, a turbulent flow is divided into two regions: the constant α region away from boundaries, and the near wall region. In the near wall region, Reynolds number scaling conditions imply that α decreases as Reynolds number increases. Away from boundaries, these scaling conditions imply α is independent of Reynolds number. Given the agreement with empirical and numerical data, our current work indicates that the Camassa-Holm equations provide a promising theoretical framework from which to understand some turbulent flows.

[1] Theoretical Division and Center for Nonlinear Studies, Los Alamos National Laboratory, Los Alamos, NM 87545

[2] Department of Mathematics, Indiana University, Bloomington, IN 47405

[3] Departments of Mathematics, Mechanical and Aerospace Engineering, University of California, Irvine, CA 92697.

[4] Institute for Geophysics and Planetary Physics, Los Alamos National Laboratory, Los Alamos, NM 87545

Introduction. Laminar Poiseuille flow occurs when a fluid in a straight channel, or pipe, is driven by a constant upstream pressure gradient, yielding a symmetric parabolic streamwise velocity profile. In turbulent states, the mean streamwise velocity remains symmetric, but is flattened in the center because of the increase of the velocity fluctuation. Although a lot of research has been carried out for turbulent channel flow, e.g. [1-6], accurate measurement of the mean velocity and the Reynolds stress profiles, in particular for flows at high Reynolds numbers, is still an experimental challenge. However, in the case of pipe flow, recent experiments for measuring the mean velocity profile have been successfully performed for moderate to high Reynolds numbers [7]. The fundamental understanding of how these profiles change as functions of Reynolds number seems to be still missing.

In wall bounded flows it is customary to define a characteristic velocity u_* and Reynolds number R_0 by $u_* = \sqrt{|\tau_0/|\rho}$ and $R_0 = du_*/\nu$, where τ_0 is the boundary shear stress, we take the density ρ to be unity, ν is the molecular viscosity of the fluid, and d is a characteristic macrolength. For instance, for channel flow d is the channel half-width, and for pipe flow d is the pipe radius. Based on experimental observation and numerical simulation, a piecewise expression of the mean velocity across the channel or the pipe has been commonly accepted [8], for which the nondimensional mean streamwise velocity, $\phi \equiv U/u_*$, is assumed to depend on $\eta \equiv u_* z/\nu$ and have three types of behavior depending on the distance away from the wall boundary, z : a viscous sublayer, in which $\phi \sim \eta$; the von Kármán-Prandtl logarithmic "law of the wall," in which $\phi(\eta) = \kappa^{-1}\ln\eta + A$, where $\kappa \simeq 0.41$ and $A \simeq 5.5$; and a power law region, in which $\phi \sim \eta^p, 0 < p < 1$. Alternatively, [9] proposes a single curve fitting over the whole region. Yet another proposal [10] is a family of power laws that fit the data away from the viscous sublayer, and has the log law as an envelope.

In this paper (a summary of which was given in [11]), we propose the viscous Camassa-Holm equations (VCHE) in (2.14) as a closure approximation for the Reynolds equations. The analytic form of our profiles based on the steady VCHE away from the viscous sublayer, but covering at least 95% of the channel, depends on two free parameters: the flux Reynolds number $R = dU_{\rm av}/\nu$ (where $U_{\rm av}$ is the streamwise velocity, averaged across the channel), and R_0. Due to measurement limitations most experimental data are contained in this region. Let us remark that we can further reduce the parameter dependence to one free parameter by using a drag law for the wall friction $D \sim R_0^2/R^2$. For the remaining part of the channel, we are unable to solve explicitly for the mean profile without further assumptions, but we do show compatibility of the steady VCHE with empirical and numerical velocity profiles in this subregion. The VCHE profiles agree well with data obtained from measurements and simulations of turbulent channel and pipe flow. For an other global approach to turbulent flows in channels and pipes displaying good theoretical profiles see [12].

1. The Euler-Poincaré equations and the Euler equations. Consider the Lagrangian comprised of fluid kinetic energy and a volume preservation constraint

$$L = \int da \left\{ \frac{1}{2}\left|\frac{d}{dt}X(t,a)\right|^2 + q(X(t,a),t)(\det X'_a(t,a) - 1) \right\} =$$
$$= \int dx \left\{ \frac{D}{2}|u(x,t)|^2 + q(x,t)(1 - D(x,t)) \right\} \ . \tag{1.1}$$

In (1.1), $X(t,a)$ is the Lagrangian trajectory of the material point starting at a at time $t = 0$, while

$$X'_a = \nabla_a X, u(x,t) = \frac{d}{dt}X(t,a) \ \text{ and } \ D(x,t) = (\det X'_a(t,a))^{-1} \ \text{ at } \ x = X(t,a) \ ; \tag{1.2}$$

moreover D satisfies the equation

$$\frac{\partial}{\partial t}D + \nabla\cdot(Du) = 0 \ . \tag{1.3}$$

The extremality conditions for u, where q is viewed as a Lagrange multiplier, are given by the Euler-Poincaré equation [13]

$$\left(\frac{\partial}{\partial t} + (u\cdot\nabla)\right)\frac{1}{D}\frac{\delta\mathcal{L}}{\delta u} + \frac{1}{D}\frac{\delta\mathcal{L}}{\delta u_j}\nabla u_j - \nabla\frac{\delta\mathcal{L}}{\delta D} = 0 \ , \tag{1.4}$$

(above and throughout we use Einstein's notation for summations) and

$$\frac{\delta\mathcal{L}}{\delta q} = 0 \ . \tag{1.5}$$

Since

$$\frac{1}{D}\frac{\delta\mathcal{L}}{\delta u} = u \ , \ \frac{\delta\mathcal{L}}{\delta D} = \frac{1}{2}u\cdot u - q \ , \ \frac{\delta\mathcal{L}}{\delta q} = 1 - D$$

the relations (1.3), (1.4), (1.5) yield the Euler equations

$$\left(\frac{\partial}{\partial t} + u\cdot\nabla\right)u = -\nabla q, \nabla\cdot u = 0 \ .$$

2. Averaged Lagrangians and the Camassa-Holm equations. In the presence of random fluctuations the Lagrangian trajectory given by $X(t,a)$ has to be augmented with fluctuations as

$$X^\sigma(t,a) = X(t,a) + \sigma(X(t,a),t) \ . \tag{2.1}$$

Here $\sigma = \sigma(x,t) = \sigma(x,t;\omega)$ is a random vector field. Thus the Lagrangian $L = L(\omega)$ becomes a random variable

$$L(\omega) = \int da \left\{ \frac{1}{2} \left| \frac{d}{dt} X^\sigma(t,a) \right|^2 + q^\sigma(X^\sigma(t,a),t)[\det(X^\sigma)'_a(t,a) - 1] \right\} . \tag{2.2}$$

In (2.2), we introduce the Eulerian velocity field,

$$u^\sigma(y,t) = \frac{d}{dt} X^\sigma(t,a) \ \text{ for } \ y = X^\sigma(t,a) . \tag{2.3}$$

Introducing (2.3), (2.2) and changing the variables a to $x = X(t,a)$ yields

$$L(\omega) = \int dx \left\{ \frac{D}{2} |u^\sigma(x + \sigma(x,t),t)|^2 + q^\sigma(x + \sigma(x,t),t)[\det((X^\sigma)'_a \circ X^{-1}) - D] \right\} ,$$

where D as before is given by (1.2) and satisfies (1.3). Noting that $(X^\sigma \circ X^{-1})(x,t) = x + \sigma(x,t)$ we conclude with

$$L(\omega) = \int dx \left\{ \frac{D}{2} |u^\sigma(x + \sigma(x,t),t)|^2 + q^\sigma(x + \sigma(x,t),t)[\det(I + \sigma'_x) - D] \right\} . \tag{2.4}$$

At this stage we make the crucial assumptions that σ is small and that the following Taylor expansions hold:

$$\begin{aligned} u^\sigma(x + \sigma(x,t),t) &\sim u(x,t) + (\sigma(x,t) \cdot \nabla) u(x,t) \\ q^\sigma(x + \sigma(x,t),t) &\sim q(x,t) + (\sigma(x,t) \cdot \nabla) q(x,t) \end{aligned} \tag{2.5}$$

where

$$\begin{aligned} u(x,t) &= \langle u^\sigma(x + \sigma(x,t),t) \rangle \\ q(x,t) &= \langle q^\sigma(x + \sigma(x,t),t) \rangle \end{aligned} \tag{2.6}$$

and $\langle \cdot \rangle$ denotes averaging with respect to the random event ω. Thus (2.4) becomes at this level of approximation

$$\begin{aligned} L(\omega) = \int dx \Big\{ & D \left[\frac{1}{2} |u(x,t)^2| + u(x,t) \cdot (\sigma(x,t) \cdot \nabla u(x,t)) + \frac{1}{2} |(\sigma(x,t) \cdot \nabla) u(x,t)|^2 \right] \\ & + [q(x,t) + (\sigma(x,t) \cdot \nabla) q(x,t)][\det(I + \sigma'_x) - D(x,t)] \Big\} . \end{aligned} \tag{2.7}$$

Therefore the averaged Lagrangian is

$$\begin{aligned} \langle L \rangle = \int dx \Big\{ & \frac{D}{2} [|u|^2 + 2u \cdot (\langle \sigma \rangle \cdot \nabla) u + \langle \sigma_i \sigma_j \rangle \partial_i u \cdot \partial_j u] + \\ & + q[\langle \det(I + \sigma'_x) \rangle - D] - D(\langle \sigma \rangle \cdot \nabla) q + (\langle \sigma \det(I + \sigma'_x) \rangle \cdot \nabla) q \Big\} , \end{aligned} \tag{2.8}$$

where we use the notation $\partial_i = \frac{\partial}{\partial x_i}, i = 1, 2, 3$. Then

$$\begin{aligned} \frac{1}{D}\frac{\delta\langle L\rangle}{\delta u} &= (1 - \frac{1}{D}\nabla\cdot(D\langle\sigma\rangle))u - \frac{1}{D}\partial_i(D\langle\sigma_i\sigma_j\rangle\partial_j u) \\ \frac{\delta\langle L\rangle}{\delta D} &= (1 + \langle\sigma\rangle\cdot\nabla)q + \frac{1}{2}[|u|^2 + 2u\cdot((\langle\sigma\rangle\cdot\nabla)u + \langle\sigma_i\sigma_j\rangle(\partial_j u)\cdot(\partial_i u)] = -Q \\ \frac{\delta\langle L\rangle}{\delta q} &= \langle\, \det(I + \sigma'_x)\rangle - D + \nabla\cdot(\langle\sigma\rangle D - \langle\sigma \det(I + \sigma'_x)\rangle)\ . \end{aligned} \tag{2.9}$$

The last equation in (2.9) becomes

$$D = \langle\, \det(I + \sigma'_x)\rangle + \nabla\cdot(\langle\sigma\rangle D) - \nabla\cdot\langle\sigma \det(1 + \sigma'_x)\rangle\ .$$

In order for the mean flow u to be incompressible, one takes $D = 1$. That gives the condition

$$1 = \langle\, \det(I + \sigma'_x)\rangle + \nabla\cdot\langle\sigma\rangle - \nabla\cdot\langle\sigma \det(I + \sigma'_x)\rangle \tag{2.10}$$

on the statistics of the fluctuations. Under this condition, the Euler-Poincaré equation (1.4) and the equation (1.3) (for $\langle L\rangle$ instead of L) can be written as

$$\frac{\partial}{\partial t}v + (u\cdot\nabla)v + v_j\nabla u_j + \nabla Q = 0\ ,\ \nabla\cdot u = 0 \tag{2.11}$$

where

$$v = (1 - \nabla\cdot\langle\sigma\rangle)u - \partial_i(\langle\sigma_i\sigma_j\rangle\partial_j u) \tag{2.12}$$

These equations are slight generalizations of the Camassa-Holm equations. The latter correspond to the case where the isotropy conditions

$$\langle\sigma\rangle = 0\ ,\ \langle\sigma_i\sigma_j\rangle = \alpha^2\delta_{ij}\ , \tag{2.13}$$

hold. If moreover the statistics are homogeneous, then α^2 is constant. Under this form the equations (2.11), (2.12) were derived in [14]. That derivation generalizes a one-dimensional integrable dispersive shallow water model studied in [15] to n-dimensions and provides the interpretation of α as the typical mean amplitude of the fluctuations. See [16] for the extension of that derivation to Riemannian manifolds.

We note that v in (2.12) represents a momentum. Therefore we propose the viscous variant of (2.11) should look as

$$\frac{\partial}{\partial t}v + (u\cdot\nabla)v + v_j\nabla u_j = \nu\Delta v - \nabla Q\ ,\ \nabla\cdot u = 0\ , \tag{2.14}$$

where v is again given by (2.12). Throughout we will refer to equation (2.14) with definition (2.12) as the viscous Camassa-Holm equations (VCHE).

Since in (2.14), σ appears at power up to 2 and we assume $|\sigma|$ to be small (at least in average), the constraint (2.10) can be given a simpler form by using the approximation

$$\begin{aligned}\langle \det(I+\sigma'_x)\rangle - 1 \sim \nabla\cdot\langle\sigma\rangle + \langle \partial_1\sigma_1\cdot\partial_2\sigma_2 - \partial_2\sigma_1\cdot\partial_1\sigma_2\rangle + \\ + \langle \partial_2\sigma_2\cdot\partial_3\sigma_3 - \partial_3\sigma_2\cdot\partial_2\sigma_3\rangle + \langle \partial_3\sigma_3\cdot\partial_1\sigma_1 - \partial_1\sigma_3\cdot\partial_3\sigma_1\rangle\ .\end{aligned}$$

Then (2.10) becomes (by neglecting the terms of degree ≥ 3 in σ)

$$\begin{aligned}\nabla\cdot\langle(\nabla\cdot\sigma)\sigma\rangle - \nabla\cdot\langle\sigma\rangle \sim \langle \partial_1\sigma_1\cdot\partial_2\sigma_2 - \partial_2\sigma_1\cdot\partial_1\sigma_2\rangle + \\ + \langle \partial_2\sigma_2\cdot\partial_3\sigma_3 - \partial_3\sigma_2\cdot\partial_2\sigma_3\rangle + \langle \partial_3\sigma_3\cdot\partial_1\sigma_1 - \partial_1\sigma_3\cdot\partial_3\sigma_1\rangle\ .\end{aligned} \tag{2.15}$$

See [17] for the corresponding derivation of equations in the form (2.14) in Generalized Lagrangian mean (GLM) theory with $\langle\sigma\rangle = 0$ and no viscosity. We note that GLM theory provides no closure.

3. Connection with Continuum Mechanics. In order to give some mechanical interpretation to these equations we rewrite (2.11) (in the case where $\langle\sigma\rangle = 0, \alpha^2 \equiv$ constant) in the equivalent 'constitutive' form

$$\frac{du}{dt} = \mathrm{div}\boldsymbol{T}\,,\ \boldsymbol{T} = -p\boldsymbol{I} + 2\nu(1-\alpha^2\Delta)\boldsymbol{D} + 2\alpha^2\dot{\boldsymbol{D}}\,, \tag{3.1}$$

with $\nabla\cdot u = 0, \boldsymbol{D} = (1/2)(\nabla u + \nabla u^T), \boldsymbol{\Omega} = (1/2)(\nabla u - \nabla u^T)$, and co-rotational (Jaumann) derivative given by $\dot{\boldsymbol{D}} = d\boldsymbol{D}/dt + \boldsymbol{D}\boldsymbol{\Omega} - \boldsymbol{\Omega}\boldsymbol{D}$, with $d/dt = \partial/\partial t + u\cdot\nabla$. In this form, one recognizes the constitutive relation for VCHE as a variant of the rate-dependent incompressible homogeneous fluid of second grade [18], [19], whose viscous dissipation, however, is modified by the Helmholtz operator $(1-\alpha^2\Delta)$. There is a tradition at least since Rivlin [20] of modeling turbulence by using continuum mechanics principles such as objectivity and material frame indifference (see also [21]). For example, this sort of approach is taken in deriving Reynolds stress algebraic equation models [22]. Rate-dependent closure models of mean turbulence have also been obtained by the two-scale DIA approach [23] and by the renormalization group methods [24].

4. Closure Ansatz. Since VCHE describe mean quantities, we propose to use (2.11) as a turbulence closure model and test this ansatz by applying it to turbulent channel and pipe flows.

For this purpose we also assume that as long as the boundary effects can be neglected, the isotropy conditions (2.13) hold. It is also appropriate to recall that the Reynolds equations are the averaged Navier-Stokes equations [8], [23]

$$\frac{\partial}{\partial t}\bar{u} + (\bar{u}\cdot\nabla)\bar{u} = \nu\Delta\bar{u} - \nabla\bar{p} - \overline{(u-\bar{u})\cdot\nabla(u-\bar{u})}, \nabla\cdot\bar{u} = 0 \tag{4.1}$$

where the upper bar denotes the ensemble average, $\bar{u}$ is the mean flow, $\bar{p}$ the mean pressure and $-\overline{((u-\bar{u})\cdot\nabla)(u-\bar{u})}$ is the divergence of the Reynolds stresses. Our ansatz asserts that:

a) $\bar{u}$ is approximatively the solution u of the VCHE with the same symmetry and boundary conditions as $\bar{u}$.

b) The Reynolds stress divergences are given by appropriate terms in the VCHE.

5. <u>The Reynolds equations for channel flows</u>. For turbulent channel flow (see, e.g., [25]), the mean velocity in (4.1) is of the form $\bar{\boldsymbol{u}} = (\bar{U}(z), 0, 0)^{tr}$, with $\bar{p} = \bar{P}(x, y, z)$ and the Reynolds equations (4.1) reduce to

$$\begin{aligned} -\nu\bar{U}'' + \partial_z\langle wu\rangle &= -\partial_x\bar{P} \ , \\ \partial_z\langle wz\rangle = -\partial_y\bar{P} \ , \ \partial_z\langle w^2\rangle &= -\partial_z\bar{P} \ , \end{aligned} \tag{5.1}$$

where $(u, v, w)^{tr} = \boldsymbol{u} - \bar{\boldsymbol{u}}$ is the fluctuation of the velocity in the infinite channel $\{(x, y, z) \in \mathbb{R}, -d \le z \le d\}$. The (1,3) component of the averaged stress tensor $T = -\bar{p}I - \overline{u\otimes u} + \nu(\nabla\bar{u} + (\nabla\bar{u})^{tr})$ is given by $\langle T_{13}\rangle = \nu\bar{U}'(z) - \langle wu\rangle$. At the boundary, the velocity components all vanish and one has the stress condition

$$\mp\tau_0 = \langle T_{13}\rangle\big|_{z=\pm d} = \nu\bar{U}'(z)\big|_{z=\pm d} \ , \tag{5.2}$$

upon using $\langle wu\rangle = 0$ at $z = \pm d$. Hence, the Reynolds equations imply $\langle wv\rangle(z) \equiv 0$ and $\bar{P} = P_0 - \tau_0 x/d - \langle w^2\rangle(z)$, with integration constant P_0.

6. <u>The VCHE for channel flows</u>. Passing to the VCHE in the channel, we denote the velocity u in (2.14) by $\boldsymbol{U}$ and seek its steady state solutions in the form $\boldsymbol{U} = (U(z), 0, 0)^{tr}$ subject to the boundary condition $U(\pm d) = 0$ and the symmetry condition $U(z) = U(-z)$. In this particular case, the steady VCHE reduces to,

$$-\nu((1-\beta')U)' + \nu(\alpha^2U')''' = -\partial_x\tilde{\pi} \ , \ 0 = -\partial_y\tilde{\pi} \ , \ 0 = -\partial_z\tilde{\pi} \tag{6.1}$$

where $\alpha^2 = \langle\sigma_3^2\rangle, \beta = \langle\sigma_3\rangle$ and $\tilde{\pi} = \pi + \int(U - \beta'U - (\alpha^2U')')U dz$.

In agreement with the statistical assumptions in the Reynolds equation, we also take the statistics of σ to be invariant under horizontal translations. As we already mentioned above, we will suppose that away from the wall, i.e. for $|z| \leq d_0$ with $0 < d_0 < d$ we have

$$\alpha(z) \equiv \alpha_0 \ , \ \beta(z) \equiv 0 \ , \tag{6.2}$$

with constants d_0 and α_0 to be determined later. The following heuristic argument may provide some help in understanding this length α_0. Clearly α and β must depend on d, τ_0, ν, z, the only physical quantities present. Dimensional analysis then implies (with two suitable functions f and g) that

$$\frac{\alpha}{d} = f\left(R_0, \frac{d-|z|}{\ell_*}\right) \ , \ \frac{\beta}{d} = g\left(R_0, \frac{d-|z|}{\ell_*}\right) \ , \tag{6.3}$$

where $d - |z|$ is the distance to the wall, while

$$R_0 = \tau_0^{1/2} d/\nu \ , \ \ell_* = d/R_0 \ , \tag{6.4}$$

i.e., R_0 is the "skin friction" Reynolds number and ℓ_* is the wall-length unit. By eliminating R_0 in (6.3) we can write

$$\frac{\alpha}{d} = h\left(\frac{\beta}{d} \ , \ \frac{d-|z|}{\ell_*}\right) \tag{6.5}$$

with some function h of two variables. Assuming that $h(0, \infty)$ exists and noticing that

$$h\left(0, \frac{d-|z|}{\ell_*}\right) = h\left(0, \frac{d-|z|}{d} R_0\right) \ ,$$

we obtain (as long as $|z| \leq d_0$) that, for R_0 large enough, the ratio

$$\frac{\alpha}{d} \equiv \frac{\alpha_0}{d} \sim h(0, \infty)$$

is independent of R_0. This heuristic prediction will be confirmed later in a more rigorous way.

Finally, let us note that due to the symmetry of the physical setting, we can also assume that

$$\sigma_3(x, y, -z, t; \omega) \equiv -\sigma_3(x, y, z, t; \omega)$$

and therefore

$$\beta(-z, t) \equiv -\beta(z, t) \ , \ \alpha(-z, t) \equiv \alpha(z, t) \ . \tag{6.6}$$

7. Realizability conditions. Recall that the statistics of σ is subjected to the condition (2.15). In the present case this takes the form

$$\begin{aligned}&\partial_3\langle(\nabla\cdot\sigma)\sigma_3\rangle-\partial_3\beta\\ &=\langle(\partial_1\partial_3\sigma_1+\partial_2\partial_3\sigma_2)\sigma_3\rangle+\langle(\partial_1\sigma_1+\partial_2\sigma_2)\cdot\partial_3\sigma_3\rangle+\frac{1}{2}\partial_3^2\alpha^2-\partial_3\beta\\ &\sim\langle\partial_1\sigma_2\cdot\partial_2\sigma_2-\partial_2\sigma_1\cdot\partial_1\sigma_2\rangle+\langle(\partial_1\sigma_1+\partial_2\sigma_2)\cdot\partial_3\sigma_3\rangle-(\langle\partial_3\sigma_2\cdot\partial_2\sigma_3\rangle+\langle\partial_1\sigma_3\cdot\partial_3\sigma_1\rangle)\ ,\end{aligned}$$

whence

$$\frac{1}{2}(\alpha^2)''-\beta'\sim\langle\partial_1\sigma_1\cdot\partial_2\sigma_2-\partial_2\sigma_1\cdot\partial_1\sigma_2\rangle\ . \tag{7.1}$$

The meaning of σ forces

$$-d-z\le\sigma_3(x,y,z,t;\omega)\le d-z\ \text{ for }\ |z|\le d\ . \tag{7.2}$$

In this case one can prove that the following conditions hold

$$-d-z\le\beta(z)\le d-z\ ,\ \alpha(z)^2\le d^2-z^2-2z\beta(z)\ \text{ for }\ |z|\le d\ . \tag{7.3}$$

Indeed, if $P=P_{z,t}$ denotes the probability distribution of $\sigma_3(z,t;\omega)$ and

$$\beta^+=\int_{\{\sigma_3\ge 0\}}\sigma_3P(d\sigma_3)\ ,\ \beta^-=\int_{\{\sigma_3<0\}}|\sigma_3|P(d\sigma_3)$$

then

$$\beta=\langle\sigma_3\rangle=\beta^+-\beta^-\ ,\ \beta^-\le(d+z)P(\{\sigma_3<0\})\ ,\ \beta^+\le(d-z)P(\{\sigma_3\ge 0\})$$

and thus

$$(d+z)^{-1}\beta^-+(d-z)^{-1}\beta^+\le 1\ ,$$

that is

$$2d\beta_-\le d^2-z^2-(d+z)\beta\ .$$

On the other hand,

$$\begin{aligned}\alpha^2=\langle\sigma_3^2\rangle=\int\sigma_3^2P(d\sigma_3)&\le(d+z)\beta^-+(d-z)\beta^+\le\\ &\le 2d\beta^-+(d-z)\beta\le d^2-z^2-2z\beta\ .\end{aligned}$$

This establishes the second inequality in (7.3). The first one is obvious.

The Cauchy-Schwarz inequality produces the supplementary constraint

$$|\beta(z)|\le\alpha(z)\ \text{for}\ |z|\le d\ . \tag{7.4}$$

It is easy to check that the conditions (7.2) and (7.4) are also sufficient for the existence of a random variable $\sigma_3(x,y,z;\omega)$ satisfying (6.6) and (7.3) and statistically depending only on z. For any such σ_3, choose some homogeneous random vector $[\sigma_1^0(x,y), \sigma_2(x,y)]$ such that $\gamma = \langle \partial_1\sigma_1^0 \cdot \partial_2\sigma_2 - \partial_2\sigma_1^0 \cdot \partial_1\sigma_2 \rangle \neq 0$. Set $\sigma_1 = (2\gamma)^{-1}\left((\alpha^2)'' - 2\beta'\right)\sigma_1^0$. Then $\sigma = (\sigma_1, \sigma_2, \sigma_3)$ has all the required statistical properties. We conclude that the inequalities (7.3) and (7.4) are the realizability conditions for the lengths α and β in the VCHE (6.1).

8. Comparing VCHE with the Reynolds equation. Comparing (5.1) and (6.1), we identify counterparts as,

$$\begin{aligned} \bar{U} = U\ ,\ \partial_z\langle wu\rangle &= \nu[(\alpha^2 U')''' - (\beta' U)''] + p_0\ , \\ \partial_z\langle wv\rangle = 0\ ,\ \nabla(\bar{P} + \langle w^2\rangle) &= \nabla(\tilde{\pi} - p_0 x)\ , \end{aligned} \tag{8.1}$$

for a constant p_0. This identification gives

$$\begin{aligned} \langle wv\rangle(z) &= 0 \\ -\langle wu\rangle(z) &= -p_0 z - \nu[(\alpha^2 U')''(z) - (\beta' U)'(z)] \end{aligned} \tag{8.2}$$

and leaves $\langle w^2\rangle$ undetermined up to an arbitrary function of z. A closure relation for $-\langle wu\rangle$ involving $U'''(z)$ also appears in Yoshizawa [23], cf. also equation (8) of [4].

From (6.1) it follows that $\partial_x\tilde{\pi} = \pi_2$ is constant. Therefore integrating twice in z, the first equation in (6.1) gives

$$-\nu(1-\beta'(z))U(z) + \nu(\alpha^2(z)U'(z))' = \pi_0 + \pi_1 z - \frac{1}{2}\pi_2 z^2 \tag{8.3}$$

with constants $\pi_i (i = 0,1,2)$. But the left hand side of (8.3) is symmetric under the change $z \mapsto -z$, so $\pi_1 = 0$ and

$$-\nu(1-\beta'(z))U(z) + \nu(\alpha(z)^2 U'(z))' = \pi_0 - \frac{1}{2}\pi_2 z^2 \ \text{ for }\ |z| \le d\ . \tag{8.4}$$

For $|z| \le d_0, \beta(z) \equiv 0, \alpha(z) \equiv \alpha_0 > 0$ and (8.4) becomes

$$-U(z) + \alpha_0^2 U''(z) = \frac{1}{\nu}\pi_0 - \frac{1}{2\nu}\pi_2 z^2 \ \text{ for }\ |z| \le d_0\ . \tag{8.5}$$

Since U is symmetric in z, we obtain

$$U(z) = a\left(1 - \frac{\cosh(z/\alpha_0)}{\cosh(d_0/\alpha_0)}\right) + b\left(1 - \frac{z^2}{d_0^2}\right) + c \ \text{ for }\ |z| \le d_0\ , \tag{8.6}$$

where the constants a, b and c satisfy the conditions

$$c = U(\pm d_0)\ ,\ \pi_0\nu = -a - b(1 + 2\alpha_0^2/d_0^2) - c\ ,\ \pi_2\nu = -2b/d_0^2\ . \tag{8.7}$$

It is worth mentioning here that with an antisymmetry condition for $U(z)$ and with (8.6) changed accordingly, we can address turbulent shear flows (Couette flows) by the same analysis as developed in this paper.

Integrating (8.4) on $[-d, 0]$ gives

$$-\nu \int_{-d}^{0} (U(z) + \beta(z)U'(z))dz - \alpha(-d)^2\tau_0 = \pi_0 d - \frac{1}{6}\pi_2 d^3 \tag{8.8}$$

where we used (5.2) as well as $U'(0) = 0, \beta(0) = 0$ and $U(-d) = 0$. Denoting

$$\begin{aligned} U_{\mathrm{av}} &= \frac{1}{2d}\int_{-d}^{d} U(z)dz = \frac{1}{d}\int_{-d}^{0} U(z)dz = \\ &= \frac{1}{d}\int_{-d}^{-d_0} U(z)dz + \left[a\left(1 - \frac{\alpha_0}{d_0}\tanh\frac{d_0}{\alpha_0}\right) + \frac{2}{3}b + c\right]\frac{d_0}{d} \end{aligned} \tag{8.9}$$

allows (8.8) to be written also as

$$-\nu d U_{\mathrm{av}} - \nu \int_{-d}^{d_0} \beta(z)U'(z)dz - \alpha(-d)^2\tau_0 = \pi_0 d - \frac{1}{6}\pi_2 d^3\ . \tag{8.10}$$

9. Empirical qualitative properties. It is universally accepted that the maximum of U is at $z = 0$ (i.e. the center of the channel) and that $U'(z) \cdot z < 0$ for $0 < |z| < d$. Also all experimental data show that $U''(z) < 0$ over most of the channel. Thus

$$R := \frac{d}{\nu}U_{\mathrm{av}} = \frac{1}{2\nu}\int_{-d}^{d} U(z)dz \le R_c \equiv \frac{d}{\nu}U(0) \tag{9.1}$$

and (using the concavity property of U)

$$R \le \frac{1}{\nu}\int_{-d}^{0}\frac{z+d}{d}U(0)dz = \frac{1}{2}R_c\ . \tag{9.2}$$

Then (9.1), (9.2) can be given the form

$$\frac{1}{2}\frac{U(0)}{u_*} \le \frac{R}{R_0} \le \frac{U(0)}{u_*}\ . \tag{9.3}$$

All the empirical evidence shows that

$$\frac{R}{R_0^2} \ll 1 \ll \frac{R}{R_0} \text{ for } R_0 \gg 1\ . \tag{9.4}$$

Throughout, the properties (9.3) and (9.4) will be taken as granted.

10. The wall units representation. In the lower half of the channel, the mean velocity U can be expressed in wall units using the notation $\phi(\eta) = U(z)/u_*, \eta = (z+d)/\ell_*$, with $\ell_* = \nu/u_* = d/R_0$. In this representation, (8.6) becomes

$$\phi(\eta) = \frac{a}{u_*}\left(1 - \frac{\cosh \xi(1-\eta/R_0)}{\cosh \xi(1-\eta_0/R_0)}\right) + \frac{b}{u_*}\left(1 - \left(\frac{1-\eta/R_0}{1-\eta_0/R_0}\right)^2\right) + \phi(\eta_0) \,, \tag{10.1}$$

for $\eta_0 \le \eta \le R_0$, where $\xi = d/\alpha$ and $\eta_0 = (d-d_0)/\ell_* \sim \alpha_0/\ell_* = R_0/\xi$.

The definition of ϕ, implies $R = \int_0^{R_0} \phi(\eta) d\eta$. Hence (10.1) gives

$$R = \frac{aR_0}{u_*}\left(1 - \frac{\tanh \xi(1-q_0)}{\xi(1-q_0)}\right) + \frac{2bR_0}{3u_*} + \phi(\eta_0)(R_0 - \eta) + \int_0^{\eta_0} \phi(\eta) d\eta \,.$$

To conclude this computation it is sufficient to approximate ϕ on $(0, \eta_0)$ by the piecewise linear function equal to η for $0 < \eta \le \eta_*$ and $\phi_0 + (\eta - \eta_0)\phi'_0$ for $\eta_* \le \eta \le \eta_0$, where $\phi_0 = \phi(\eta_0), \phi'_0 = \phi'(\eta_0)$ and $\eta_* = (\phi_0 - \eta_0\phi'_0)/(1-\phi'_0)$. We obtain

$$\frac{R}{R_0} \approx \frac{a}{u_*}\left(1 - \frac{\tanh \xi(1-q_0)}{\xi(1-q_0)}\right) + \frac{2b}{3u_*} + (1-q_0)\phi_0 + (1-\phi'_0)^{-1}\left(\phi_0 q_0 - \frac{q_0^2 R_0 \phi'_0 + \phi_0^2/R_0}{2}\right) \tag{10.2}$$

where

$$\phi'_0 = (a/u_*)(\xi/R_0)\tanh(\xi(1-q_0)) + 2(b/u_*)/R_0(1-q_0) \,. \tag{10.3}$$

Using this and solving for ϕ_0 gives an explicit function $\phi_0 = \phi_0(q_0; R, R_0; a/u_*, b/u_*; \xi)$, namely

$$\phi_0(q_0; R, R_0; a/u_*, b/u_*; \xi) = R_0\left\{B - \sqrt{B^2 - \frac{1}{R_0}[2(R/R_0 - C) + q_0^2 R_0 \phi'_0]}\right\} \tag{10.4}$$

where ϕ'_0 is given by (10.3),

$$B = (1-q_0)(1-\phi'_0) + q_0$$
$$C = \frac{a}{u_*}\left(1 - \frac{\tanh \xi(1-q_0)}{\xi(1-q_0)}\right) + \frac{2}{3}\frac{b}{u_*} \tag{10.5}$$

and the choice of the root ϕ_0 in (10.2), (10.3) will be justified at the end of Section 11.

Thus (10.1) becomes

$$\phi(\eta) = \frac{a}{u_*}\left(1 - \frac{\cosh\xi(1-\eta/R_0)}{\cosh\xi(1-q_0)}\right) + \tag{10.6}$$
$$+ \frac{b}{u_*}\left(1 - \left(\frac{1-\eta/R_0}{1-q_0}\right)^2\right) + \phi_0(q_0; R, R_0; \frac{a}{u_*}, \frac{b}{u_*}; \xi) \text{ for } q_0 R_0 \le \eta \le R_0 .$$

In (10.6) the constants $a/u_*, b/u_*, \xi$ and q_0 may depend on R_0. As we will show below, Nature seems to choose them as constants (at least for large R_0). Recall that in Section 6 we already gave a heuristic argument that $\xi = d/\alpha$ should be independent of R_0 if R_0 (or R) is large enough.

11. The off wall region. The empirical data up to now suggest that for a fixed channel there is a range (z_1, z_2) (with $z_1 z_2 > 0$) inside the channel such that for z in that range, the von Kármán log-law is a good approximation to $U(z)$, at least for R (or R_0) large enough. Since for those z we have

$$U(z_2) - U(z) = \frac{1}{\kappa}\ln\frac{z_2}{z} = \frac{1}{\kappa}\left(\ln\frac{z_2}{d} - \ln\frac{z}{d}\right)$$

(where $\kappa \sim .4$ is the von Kármán constant), $U(z_2) - U(z)$ is a function of z/d only (i.e. independent of R_0). We will posit now the following weaker condition.

For R (or R_0) large enough, there exists a fixed range $(z_1/d, z_2/d)$ such that for z/d in that range, $U(z_2) - U(z)$ is a function of z/d, independent of R_0.

Note that we make no assumption on the length of the range. The classical "defect law" of Izakson, Millikan and von Mises [26] (pp. 186–188) is the particular case of our condition when one of z_i's is 0, and the range is assumed to be wide.

Passing to the wall units representation we can formulate our assumption as: There exists $0 < q_1 < q_2 < 1$, such that for $q_1 R_0 \le \eta \le q_2 R_0, \phi(\eta_2) - \phi(\eta)$ is a function of $q = \eta/R_0$ only. Since we expect q_0 in (10.6) to be quite small, we will take $q_0 \le q_1$.

We will prove now that under the above conditions, there exist absolute constants a_*, b_* and ξ_* such that

$$a \sim a_* u_* \cosh\xi_*(1-q_0)\ ,\ b \sim b_* u_*(1-q_0) \text{ and } \xi = d/(\alpha_0 \xi_*) \tag{11.1}$$

where a, b, ξ and q_o are as in (10.6).

Indeed let f be the function defined by

$$f(q) = \phi(q_2 R_0) - \phi(q R_0) \text{ for } q_1 \le q \le q_2 . \tag{11.2}$$

Then since $q_0 \leq q_1$ we have from (10.6)

$$f(q) = a_0[\cosh\xi(1-q) - \cosh\xi(1-q_2)] + b_0[(1-q)^2 - (1-q_2)^2] \tag{11.3}$$

where

$$a_0 = (a/u_*)/\cosh\xi(1-q_0)\ ,\ b_0 = (b/u_*)/(1-q_0)^2\ . \tag{11.4}$$

Writing (11.3) for $q = q_1$, we obtain

$$b_0 = \frac{f(q_1) - a[\cosh\xi(1-q_1) - \cosh\xi(1-q_2)]}{(1-q_1)^2 - (1-q_2)^2}\ .$$

Then (11.3) becomes

$$a_0 g(\xi, q) = h(q) \ \text{ for } \ q_1 \leq q \leq q_2 \tag{11.5}$$

where, with c_0, c_1 absolute constants,

$$\begin{aligned} q(\xi, q) &= \cosh\xi(1-q) - \cosh\xi(1-q_2) - c_1[(1-q)^2 - (1-q_2)^2] \\ h(\xi) &= f(q) - c_0[(1-q)^2 - (1-q_2)^2]\ , \end{aligned} \tag{11.6}$$

and a_0, ξ are parameters, constant in q but which may depend continuously on R_0. Note that

$$g(\xi, q_i) = h(q_i) = 0\ (i = 1, 2)\ ,\ g(\xi, q) < 0 \ \text{ for } \ q_1 < q < q_2\ ,\ \xi > 0\ . \tag{11.7}$$

Thus

$$a_0 = h\left(\frac{q_1 + q_2}{2}\right) g\left(\xi, \frac{q_1 + q_2}{2}\right) \tag{11.8}$$

and

$$g(\xi, q) h\left(\frac{q_1 + q_2}{2}\right) = h(q) g\left(\xi, \frac{q_1 + q_2}{2}\right) \ \text{ for } \ q_1 \leq q \leq q_2\ . \tag{11.9}$$

If $\xi = \xi(R_0)$ is not constant then (11.9) would hold for ξ in an interval $[\xi_1, \xi_2], 0 < \xi_1 < \xi_2$. Differentiating (11.9) with respect to ξ gives

$$g'_\xi(\xi, q) g\left(\xi, \frac{q_1 + q_2}{2}\right) = g'_\xi\left(\xi, \frac{q_1 + q_2}{2}\right) g(\xi, q)$$

for $\xi_1 \leq \xi \leq \xi_2, q_1 \leq q \leq q_2$. Taking $q = q_1$ gives $g'_\xi(\xi, q_1) = 0$ for $\xi_1 \leq \xi \leq \xi_2$, that is

$$\sinh\xi(1-q_1) - \sinh\xi(1-q_2) = 0 \ \text{ for } \ \xi_1 \leq \xi < \xi_2$$

which is impossible.

We conclude that there are absolute constants q_0, a_*, b_* and ξ_* such that

$$\begin{aligned}\phi(\eta) = {} & a_* \left[\cosh \xi_*(1-q_0) - \cosh \xi_* \left(1 - \frac{\eta}{R_0}\right)\right] + \\ & + b_* \left[(1-q_0)^2 - \left(1 - \frac{\eta}{R_0}\right)^2\right] + \\ & + \phi_0(q_0; R, R_0; a_* \cosh \xi_*(1-q_0), b_*(1-q_0)^2; \xi_*) \end{aligned} \tag{11.10}$$

for $q_0 R_0 \le \eta \le R_0$, where the function ϕ_0 (see (10.4)) is actually depending only on q_0, R_0 and R.

The formula (11.10) can be also written as

$$\phi(qR_0) = \phi_1(q_0; q) + \phi_0(q_0; R, R_0) \ \text{ for } \ q_0 \le q \le 1 \tag{11.11}$$

where

$$\begin{aligned}\phi_1(q_0; q) = {} & a_* \cosh \xi_*(1-q_0) \left(1 - \frac{\cosh \xi(1-q)}{\cosh \xi(1-q_0)}\right) + \\ & + b_*(1-q_0)^2 \left(1 - \left(\frac{1-q}{1-q_0}\right)^2\right) \ \text{ for } \ q_0 \le q \le 1 \ , \\ \phi_0(q_0; R, R_0) = {} & \phi_0(q_0; R, R_0; a_* \cosh \xi_*(1-q_0), b_*(1-q_0)^2; \xi_*) \ . \end{aligned} \tag{11.12}$$

For $R_0 \to \infty$ from (10.4) and (10.5) we have

$$\phi(q_0 r_0) = \phi_0(q_0; R, R_0) \sim \frac{R}{R_0} - C + \frac{1}{2} q_0^2 C_0 \ , \tag{11.13}$$

where C is defined in (10.5) and $C_0 = R_0 \phi_0'$ is constant according to (10.3).

We can now explain the choice of ϕ_0 in (10.4). The other possible choice was

$$R_0 \left[B + \sqrt{B^2 \frac{1}{R_0} \{2(R/R_0 - C) + q_0^2 C_0\}}\right]$$

which would have given for R_0 large enough

$$\phi(q_0 R_0) \sim 2R_0$$

and consequently $\phi(R_0) \ge R_0$ which is contrary to the established facts (9.3), (9.4).

12. The mean velocity profile in the channel. Comparing the profile given by formula (11.10) with an experimental mean velocity profile, enables us to obtain the values a_*, b_* and ξ_* as well as the smallest acceptable value q_* for q_0. In Figure 1, we compare our formula with experimental data [4] for the Reynolds numbers R_0 equal to 714, 989, and 1608. As these Reynolds numbers are small, a_* and b_* have not reached their asymptotic values. It appears, however, that ξ_* has reached its asymptotic value. We therefore allow a_* and b_* to vary slightly while holding ξ_* constant to fit the data. It turns out that $\xi_* = 35$ and $q_* = 1/\xi_*$. Note that this choice of q_* corresponds exactly to the condition that $|d - d_0| = \alpha$.

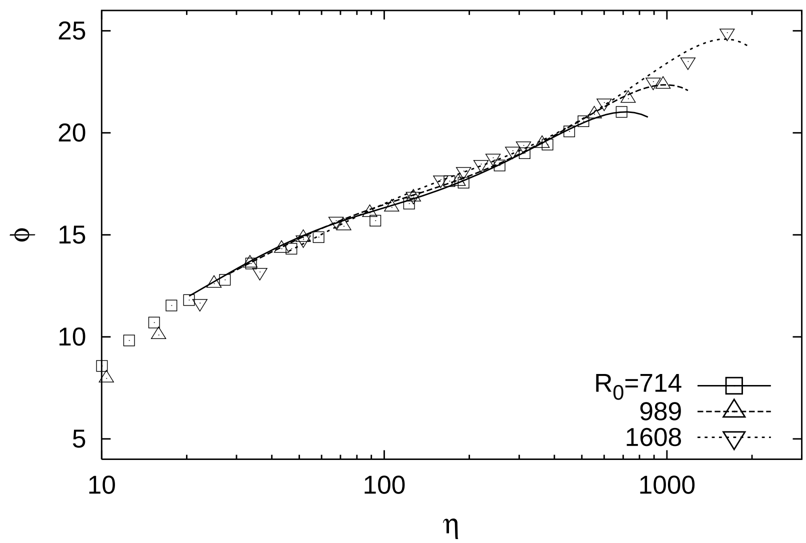

FIG. 1. The mean velocity profile in the channel for the constant-α viscous Camassa-Holm equation compared with the experimental data of Wei and Willmarth [4].

13. The Reynolds shear stress. The shear Reynolds stress is $-\langle uw \rangle$ (see Section 5). Since $\langle uw \rangle\big|_{z=\pm d} = 0$, one must have

$$-\langle uw \rangle(z) = -\tau_0 \frac{z}{d} - \nu \bar{U}'(z) \quad \text{for} \quad |z| \leq d\,. \tag{13.1}$$

On the other hand $\bar{U} \equiv U$ and $-\langle uw \rangle$ is also given by (8.2) with an appropriate constant p_0. For $|z| \leq d_0$, since $\alpha(z) \equiv \alpha_0 = 1/\xi_*, \beta(z) \equiv 0$, (8.2) reduces to

$$-\langle uw \rangle(z) = p_0 z - \nu \alpha_0^2 U'''(z) \tag{13.2}$$

and

$$\nu \alpha_0^2 U'''(z) = \nu U'(z) - \pi_2 z \ .$$

Introducing this in (13.2) we see that (13.1) and (13.2) are compatible if p_0 is given by

$$p_0 = -\pi_0 - \tau_0/d \ . \tag{13.3}$$

Taking the wall units representation in (13.1) we obtain our theoretical Reynolds shear stress

$$\frac{-\langle uw \rangle}{\tau_0} = 1 - \frac{\eta}{R_0} - \phi'(\eta) =$$
$$= 1 - \frac{\eta}{R_0} + \frac{a_*}{R_0}\xi_* \sinh \xi_* \left(1 - \frac{\eta}{R_0}\right) + \frac{2b_*}{R_0}\left(1 - \frac{\eta}{R_0}\right) \quad \text{for} \quad q_* R_0 \le \eta \le R_0 \ . \tag{13.4}$$

Figure 2 compares the corresponding experimental and theoretical Reynolds shear stresses. We use the same values for a_*, b_* and ξ_* as before. The shear stresses do not extend so close to the wall as the mean velocity profiles did. The empirical matching of the mean velocity profiles as well as the Reynolds shear stresses works with $q_* = \sqrt{3}/\xi_*$.

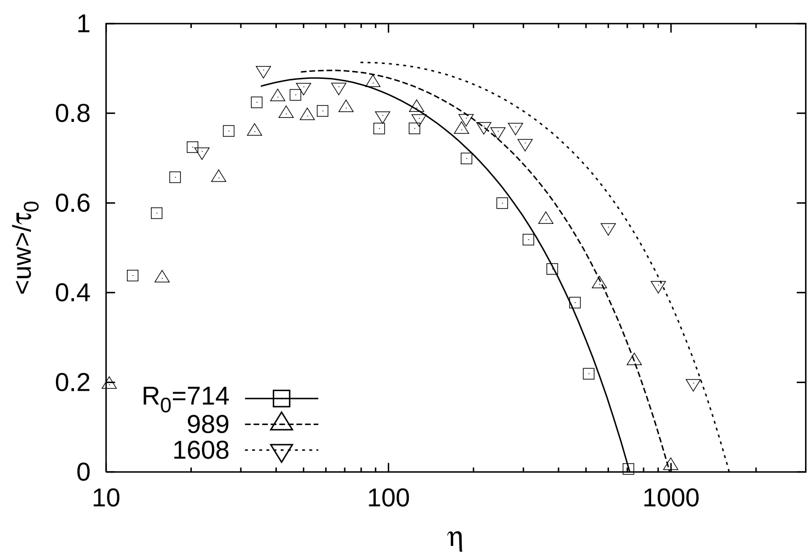

FIG. 2. Reynolds shear stress in the channel compared with the experimental data in [4].

14. <u>The near wall region</u>. As already mentioned above, in the near wall regions (i.e. where $0 \le \eta \le \eta_0 = q_* R_0$ and $2R_0 - q_* R_0 \le \eta \le 2R_0$), β may be non-zero and α may depend

(as does β) on η and R_0. The VCHE (8.4) in the wall units representation takes the form

$$(1 - R_0\tilde{\beta}'(\eta))\phi(\eta) - R_0^2(\tilde{\alpha}(\eta)^2\phi'(\eta))' = f_0 + 3f_1\left(1 - \frac{\eta}{R_0}\right)^2$$
$$\text{for } \ 0 \le \eta \le R_0 \tag{14.1}$$

i.e., in the whole lower half of the channel. In (14.1) we used the notations

$$\tilde{\alpha}(\eta) = \alpha(z)/d \ , \ \tilde{\beta}(\eta) = \beta(z)/d \tag{14.2}$$

where $d + z = \eta\ell_*, \ell_* = d/R_0$, and

$$\begin{aligned} f_0 &= -\pi_0/\nu u_* = a_* \cosh \xi_*(1 - q_*) + b_*\left[(1 - q_*)^2 + \frac{2}{\xi_*^2}\right] + \phi(q_* R_0) \\ f_1 &= \pi_2 d^2/\nu u_* = -b_*/3 \end{aligned} \tag{14.3}$$

Of course we have

$$\tilde{\alpha}(\eta) = 1/\xi_* \ , \ \tilde{\beta}(\eta) = 0 \ \text{ for } \ q_* R_0 \le \eta \le R_0 \ , \tag{14.4}$$

but the VCHE (14.1) does not define $\tilde{\alpha}(\eta), \tilde{\beta}(\eta)$ near the wall (i.e. for $0 \le \eta \le q_* R_0$). However, (14.1) gives some qualitative information on the behavior of $\tilde{\alpha}$ and $\tilde{\beta}$ in the near wall region. Indeed integrating (14.1) we obtain

$$\begin{aligned} &\frac{1}{R_0}\int_\eta^{R_0} \phi(\eta')d\eta' + \int_\eta^{R_0} \tilde{\beta}(\eta')\phi'(\eta')d\eta' + \tilde{\beta}(\eta)\phi(\eta) + R_0\tilde{\alpha}(\eta)^2\phi'(\eta) = \\ &= f_0\left(1 - \frac{\eta}{R_0}\right) + f_1\left(1 - \frac{\eta}{R_0}\right)^3 \end{aligned} \tag{14.5}$$

for all $0 \le \eta \le R_0$. Thus (using $|\tilde{\beta}| \le 2$, see(7.3))

$$\tilde{\alpha}(\eta)^2\phi'(\eta) \le \frac{1}{R_0}(f_0 + f_1 + 4\phi(\eta)) = O\left(\frac{R}{R_0^2}\right)$$

which in turn goes to zero when $R_0 \to \infty$, by virtue of (9.4). Thus, for η fixed,

$$\tilde{\alpha}(\eta)^2\phi'(\eta) \to 0 \ \text{ for } \ R_0 \to \infty \ . \tag{14.6}$$

In particular, (using $\phi'(0) = 1$ and (9.3))

$$\tilde{\alpha}(0) \to 0 \ , \ \tilde{\beta}(0) \to 0 \ \text{ for } \ R_0 \to \infty \tag{14.7}$$

and, due to (14.4),

$$\phi'(q_* R_0) \to 0 \ \text{ for } \ R_0 \to \infty \ . \tag{14.8}$$

Moreover, writing (14.5) for $\eta = 0$,

$$\frac{R}{R_0} + \int_0^{R_0} \tilde{\beta}(\eta')\phi'(\eta')d\eta' + R_0 \tilde{\alpha}(0)^2 = f_0 + f_1 \tag{14.9}$$

and subtracting (14.5) from (14.9) we obtain

$$\frac{1}{R_0}\int_0^{\eta} \phi(\eta')d\eta' + \int_0^{\eta} \tilde{\beta}(\eta')\phi'(\eta')d\eta' - \tilde{\beta}(\eta)\phi(\eta) + R_0[\tilde{\alpha}(0)^2 - \tilde{\alpha}(\eta)^2\phi'(\eta)] =$$
$$= f_0\frac{\eta}{R_0} + f_1\left[1 - \left(1 - \frac{\eta}{R_0}\right)^3\right] \tag{14.10}$$

Fixing η and letting $R_0 \to \infty$, from (14.10) we infer that

$$\int_0^{\eta} \tilde{\beta}(\eta')\phi'(\eta')d\eta' - \tilde{\beta}(\eta)\phi(\eta) + R_0[\tilde{\alpha}(0)^2 - \tilde{\alpha}(\eta)^2\phi'(\eta)] \to 0 \ . \tag{14.11}$$

But for η fixed such that $\phi'(\eta)$ remains away from 0 when $R_0 \to \infty$, we have $\beta(\eta) \to 0$ because of (7.4). By virtue of Lebesgue's dominated convergence theorem we conclude that

$$R_0[\tilde{\alpha}(0)^2 - \tilde{\alpha}(\eta)^2\phi'(\eta)] \to 0 \ \text{ when } \ R_0 \to \infty \tag{14.12}$$

provided that $\phi'(\eta)$ stays away from 0.

It is instructive to connect (14.12) with the functions g and h considered in Section 6. First we recall that

$$g(R_0, \eta) = \tilde{\beta}(\eta) \ , \ f(\tilde{\beta}(\eta), \eta) = \tilde{\alpha}(\eta) \tag{14.13}$$

Assuming that $\tilde{\beta}$ and $\tilde{\beta}'$ are continuous across $\eta_0 = q_* R_0$, we obtain

$$g(R_0, R_0 q) = -\int_q^{q_*} (q' - q_*)\Big(\frac{\partial}{\partial q'}\Big)^2 g(R_0, R_0 q')dq' \ \text{ for } \ 0 \le q \le q_* \ .$$

Since q_* is small, assuming that

$$\left[\Big(\frac{\partial}{\partial q'}\Big)^2 g(R_0, R_0 q')\right]\Bigg|_{q' = q_* - 0} = \gamma(R_0)$$

exists and is not zero, we obtain that

$$g(R_0, \eta) \sim \frac{1}{2}\gamma(R_0)(q_* - \eta/R_0)^2 \ . \tag{14.14}$$

But $\tilde{\beta}(0) \geq 0$, so $\gamma(R_0) > 0$. If $\gamma(R_0) = 0$, we can proceed in a similar way by involving a higher derivative of g at η_0 from the left. In all cases we have ended with a representation

$$g(R_0, \eta) \sim g_0(R_0) g_1(\eta/R_0) \text{ for } 0 \leq \eta \leq q_* R_0 \tag{14.15}$$

where $g_0 \geq 0, g_1 \geq 0$ and $g_1(q)$ is a decreasing function of q with $g_1(q_*) = g_1'(q_*) = 0$. From (14.15), (14.13) and (14.12) we now obtain

$$h^2(g_0(R_0)g_1(0), 0) - h^2(g_0(R_0)g_1(\eta/R_0), \eta)\phi'(\eta) \sim 0 \tag{14.16}$$

for R_0 large enough. In (14.16), $g_1(\eta/R_0) \to g_1(0)$ for $R_0 \to \infty$ and η fixed. These arguments suggest that

$$h(\beta, \eta) \sim h(\beta, 0)/\sqrt{\phi'(\eta)} \tag{14.17}$$

provided β is small and $1/\phi'(\eta)$ is bounded when $R_0 \to \infty$. It is not clear if assuming equality in (14.17) is a judicious approximation of the function h.

A major difficulty in fine tuning our approach near the wall resides in the unavailability of experimental data in the near wall region for large Reynolds numbers. To test whether the VCHE (14.5) is still valid in this region we extrapolated the experimental profiles in Figure 1 into the near wall region according to Panton [9] to obtain α from (13.5). For simplicity of the graph, we will display the α profile only for $R_0 = 1608$, which is the highest Reynolds number in Figure 1. As illustrated in Figure 3, we find that the realizability conditions (in Section 7) are satisfied for appropriate choice of $\gamma(R_0)$ in (14.14) and (14.13). Clearly α lies between the upper constraint (7.3) and the lower constraint (7.4) in the near wall region. Thus, our basic ansatz is consistent with Panton's theory.

15. Pipe flows and prediction. All the preceding considerations on turbulent channel flows can be suitably applied to turbulent pipe flows. The substantial difference between the mathematical treatment of the two types of flows, is that for pipes, the cosh function is replaced by the first modified Bessel function (see [27])

$$I_0(r) = \sum_{n=1}^{\infty} \frac{1}{(n!)^2} \left(\frac{r^2}{4}\right)^n . \tag{15.1}$$

For instance the basic formula (10.11) becomes

$$\begin{aligned}\phi(\eta) = \frac{a}{u_*}\left[1 - \frac{I_0(\xi(1-\eta/R_0)}{I_0(\xi(1-\eta_0/R_0)}\right] + \frac{b}{u_*}\left(1 - \left(\frac{1-\eta/R_0}{1-\eta_0/R_0}\right)^2\right) \\ + \phi(\eta_0) \text{ for } \eta_0 \leq \eta \leq R_0 .\end{aligned} \tag{15.2}$$

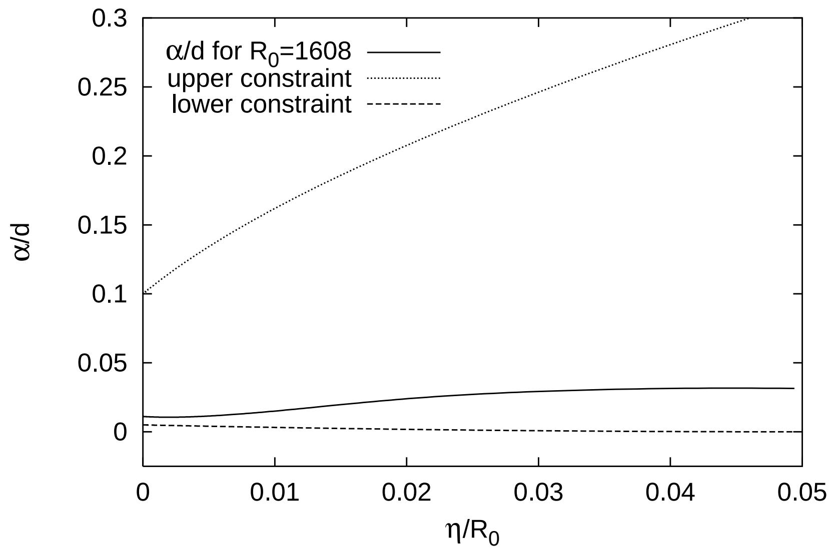

FIG. 3. The statistical compatibility of the VCHE with Panton's theory [9] in the near wall region.

For pipe flows, experimental data for quite large Reynolds numbers are available (e.g. [7]). For these Reynolds numbers it is reasonable to assume that a_*, b_*, and ξ_* have each reached their asymptotic values. In Figure 4 we compare our profiles with experimental data [7]. We obtain the a_*, b_*, ξ_* and q_* by using the experimental data for $R = 98,812$ and use the von Kármán drag law, $R/R_0 \sim \log R_0$, to obtain profiles for $R = 3,089,100$ and $35,259,000$.

We note that our predictions are consistent with the von Kármán log law [28], the Barenblatt-Chorin power law [10], as well as with the presence of the 'chevron' near the center of the flow. Our approach shows a logarithmic profile for $0.02\ R_0 \leq \eta \leq 0.2 R_0$ and a chevron near the center of the channel. The Barenblatt-Chorin power law [10] may represent the transition in the profile from the log law to the chevron. Although our approach is in good agreement with the experiments [7], we note that in [10] it is argued that the experimental mean velocity profiles are too low for high Reynolds numbers. Finally, we observe that the chevron may reflect the fact that, on the attractor of the dynamical system in the phase space of the turbulent flow, the Poiseuille-Hagen flow is recurrent.

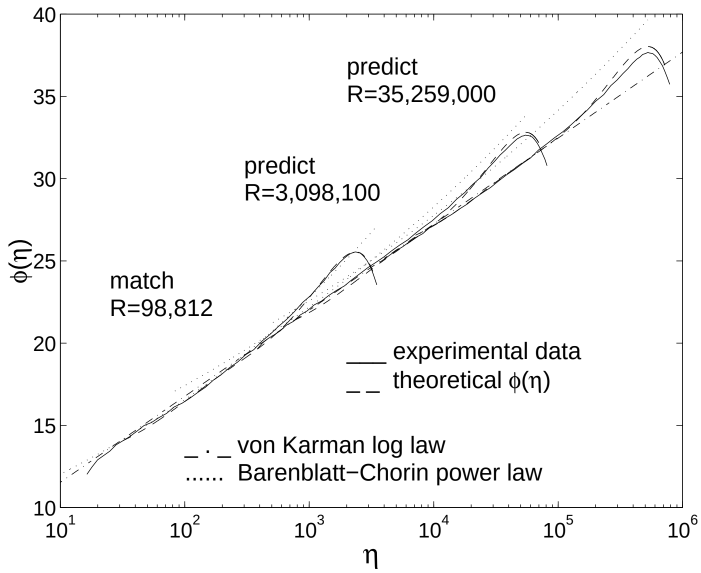

FIG. 4. The mean velocity profile in the pipe for the constant-α viscous Camassa-Holm equation compared with the experimental data of Zagarola [7].

References

[1] H. Reichardt, *Messungen turbulenter Schwankungen*, Die Naturwissenschaften **24/25** (1938), 404–408.

[2] H. Eckelmann, *Experimentelle Untersuchungen in einer turbulenten Kanalströmung mit starken viskosen Wandschichten*, Mitteilungen aus dem Max-Planck-Institut für Strömungsforschung und der Aerodynamischen Versuchsanstalt, Göttingen, no. 48 (1970).

[3] H. Eckelmann, *The structure of the viscous sublayer and the adjacent wall region in a turbulent channel flow*, J. Fluid Mech., **65** (1974), 439–459.

[4] T. Wei and W.W. Willmarth, *Reynolds-number effects on the structure of a turbulent channel flow*, J. Fluid Mech., **204** (1989), 57–95.

[5] R.A. Antonia, M. Teitel, J. Kim and L.W.B. Browne, *Low-Reynolds-number effects in a fully developed turbulent channel flow*, J. Fluid Mech., **236** (1992), 579–605.

[6] J. Kim, P. Moin and R. Moser, *Turbulence statistics in fully developed channel flow at low Reynolds number*, J. Fluid Mech., **177** (1987), 133–166.

[7] M.V. Zagarola, *Mean-Flow Scaling of Turbulent Pipe Flow*, Ph.D thesis, Princeton University (1996).

[8] J.O. Hinze, *Turbulence*, Mc-Graw-Hill: New York, 2nd edition (1975).

[9] R.L. Panton, *A Reynolds Stress Function for Wall Layers*, J. of Fluids Eng., **119** (1997), 325–329.

[10] See, e.g. G.I. Barenblatt, A.J. Chorin and V.M. Prostokishin, *Scaling laws for fully*

developed turbulent flow in pipes, Appl. Mech. Rev., **50** (1997), 413, for a recent survey of pipe flows and G.I. Barenblatt and A.J. Chorin, *Scaling laws and vanishing viscosity limits in turbulence theory*, SIAM Rev., **40**,No. 2, (1998), 265.

[11] S. Chen, C. Foias, D.D. Holm, E. Olson, E.S. Titi, S. Wynne, *The Camassa-Holm equations as a closure model for turbulent channel and pipe flow*, Phys. Rev. Lett. (submitted).

[12] W.V.R. Malkus, L.M. Smith, *Upper bounds on functions of the dissipation rate in turbulent shear flow*, J. Fluid Mech., vol. **208** (1989), 479–507.

[13] D.D. Holm, J.E. Marsden, T.S. Ratiu, *The Euler-Poincare Equations in Geophysical Fluid Dynamics*, (see section 3).

[14] D.D. Holm, J.E. Marsden, T.S. Ratiu, *Euler-Poincare Models of Ideal Fluids with Nonlinear Dispersion*, Phys. Rev. Lett., **80** (1998), 4173.

[15] R. Camassa and D.D. Holm, Phys. Rev. Lett., *An integrable shallow water equation with peaked solitons*, **71** (1993), 1661–1664.

[16] D.D. Holm, S. Kowanbaeva, J.E. Marsden, T. Ratiu and S. Shkoller, *Arnol'd Festshrift*, vol.**2** (to appear).

[17] I. Gjaja and D.D. Holm, *Self-consistent Hamiltonian dynamics of wave mean-flow interaction for a rotating stratified incompressible fluid*, Physica D, **98** (1996), 343–378.

[18] J.E. Dunn and R.L. Fosdick, *Thermodynamics, Stability, and Boundedness of Fluids of Complexity 2 and Fluids of Second Grade*, Arch. Rat. Mech. Anal., **56** (1974), 191–252.

[19] J.E. Dunn and K.R. Rajagopal, *Fluids of Differential Type: Critical Reviews and Thermodynamic Analysis*, Int. J. Engng. Sci., **33** (1995), 689–729.

[20] R.S. Rivlin, *The Relation Between the Flow of Non-Newtonian Fluids and Turbulent Newtonian Fluids*, Q. Appl. Math., **15** (1957), 212–215.

[21] A.J. Chorin, *Spectrum, Dimension, and Polymer Analogies in Fluid Turbulence*, Phys. Rev. Lett. **60** (1988), 1947–1949.

[22] T.H. Shih, J. Zhu and J.L. Lumley, *A New Reynolds Stress Algebraic Equation Model*, Comput. Methods Appl. Mech. Engng., **125** (1995), 287–302.

[23] A. Yoshizawa, *Statistical Analysis of the Derivation of the Reynolds Stress from its Eddy-viscosity Representation*, Phys. Fluids, **27** (1984), 1377–1387.

[24] R. Rubinstein and J.M. Barton, *Nonlinear Reynolds Stress Models and the Renormalization Group*, Phys. Fluids A, **2** (1990), 1472–1476.

[25] A.A. Townsend, *The Structure of Turbulent Flows*, Cambridge University Press (1967).

[26] J.L. Lumley and H. Tennekes,*A First Course in Turbulence*, MIT Press (1972).

[27] M. Abramowitz and I.A. Stegun, *Handbook of Mathematical Functions*, Dover Publications, Inc., New York, 9th edition.

[28] L.D. Landau and E.M. Lifshitz, *Fluid Mechanics*, Pergamon Press, 2nd edition (1987).